

MHD peristaltic transport of a micropolar fluid in an asymmetric channel with porous medium

K. V. V. Satyanarayana¹, S. Sreenadh¹, P. Lakshminarayana^{2*} and G. Sucharitha²

¹Department of Mathematics, Sri Venkateswara University, Tirupati, India

²Department of Mathematics, Sree Vidyanikethan Engineering College, Tirupati, India

ABSTRACT

In the present study the peristaltic transport of an incompressible conducting micropolar fluid in an asymmetric channel with porous medium has been studied under the assumptions of long wave length and low Reynolds number. Applying wave frame analysis, exact analytical solutions have been obtained for the axial velocity and the microrotation component. Expression for the pressure rise is also obtained. The influence of physical parameters on the velocity, pressure gradient and pressure rise are presented through graphs. The effect of increase in the permeability parameter and the magnetic parameter is to reduce the velocity.

Keywords: Peristaltic Transport, micropolar fluid, MHD, Porous medium, Asymmetric channel.

INTRODUCTION

Peristaltic transport is a mechanism of fluid transport which occurs when a progressive wave of area contraction or expansion propagates along the distensible tube containing fluid. The principle of peristalsis is used for pumping physiological fluids from one place to another in a living body, such as swallowing food through the esophagus, the transport of spermatozoa in the ductus efferentes of the male reproductive tract, movement of chyme in the gastrointestinal tract, urine transport from the kidneys to the urinary bladder through the ureter, movement of ovum in the fallopian tubes, bile flow from the gall bladder into the duodenum and circulation of blood in small blood vessels. Also many practical applications involve in modern biomedical and mechanical systems such as blood pump machine, heart-lung machine, dialysis machine and noxious fluid transport in nuclear industries.

Most of the physiological fluids behave like a non-Newtonian fluids. Hence the peristaltic transport of non-Newtonian fluids have much attention recently. Among several non-Newtonian models proposed for physiological fluids, micropolar fluid has considerable interest due to its importance in engineering and biomedical problems. After the first investigation of Eringen [1], this model attracted the attention of many researchers. Lukaszewicz [2] gives many important aspects of the theory and applications of micropolar fluids. A few investigators considered the peristaltic flow problems concerning these fluids. Srinivasacharya et al. [3] analyzed the peristaltic transport of a micropolar fluid in a tube. Ali and Hayat [4] discussed the peristaltic flow of a micropolar fluid in an asymmetric channel.

Hayat et al. [5] studied the peristaltic flow of a micropolar fluid in a channel with different wave forms. Sreenadh et al. [6] investigated the peristaltic flow of micropolar fluid in an asymmetric channel with permeable walls. The influence of partial slip on the peristaltic transport of a micropolar fluid in an inclined asymmetric channel is studied by Arun Kumar et al. [7].

Magneto hydrodynamics is the dynamics of electrically conducting fluids. It is now a well accepted fact that the peristaltic flows of magnetohydrodynamic fluids are important in medical sciences and bioengineering. The mutual interaction between the fluid motion and magnetic field is the essential feature of the physical situation in the MHD

fluid flow problems. MHD principles are useful in the design of heat exchangers, pumps, radar systems, power generation development of magnetic devices, cancer tumor treatment, hyperthermia and blood reduction during surgeries. It is realized that the principles of magneto hydrodynamics find extensive applications in bioengineering and medical sciences. Hence several scientists having in mind such importance extensively discussed the peristalsis with magnetic field effects [8-15].

The study of fluid flows through porous medium has attracted much attention recently. This is primarily because of practical applications of flow through porous media, such as separation process in chemical industries, filtration, transpiration cooling, storage of radioactive nuclear waste material transfer, transport process in aquifers and ground water pollution. Several researchers studied the peristaltic flow with porous media [16-23].

In this paper the influence of MHD on peristaltic transport of an incompressible micropolar fluid in an asymmetric channel with porous medium has been investigated under the assumptions of long wave length and low Reynolds number. The expression for the velocity, pressure rise are obtained. The effects of different parameters on velocity, pressure gradient and pressure rise are discussed through graphs.

2. Mathematical formulation

Consider the flow of an incompressible micropolar fluid in a two dimensional porous asymmetric channel of width $d_1 + d_2$, in the presence of a magnetic field. The flow in the channel is governed by micropolar model and is induced by sinusoidal wave trains propagating with constant speed C along the channel wall. The geometry of the walls surfaces is given by

$$\bar{h}_1(\bar{x}, \bar{t}) = d_1 + a_1 \cos\left(\frac{2\pi}{\lambda}(\bar{x} - c\bar{t})\right) \quad (\text{right hand side wall}) \quad (1)$$

$$\bar{h}_2(\bar{x}, \bar{t}) = -d_2 - a_2 \cos\left(\frac{2\pi}{\lambda}(\bar{x} - c\bar{t}) + \phi\right) \quad (\text{left hand side wall}) \quad (2)$$

where a_1 and a_2 are the amplitudes of the waves, λ is the wave length, C is the wave speed, ϕ ($0 \leq \phi \leq \pi$) is the phase difference, \bar{X} and \bar{Y} are the rectangular coordinates with \bar{X} measured along the axis of the channel and \bar{Y} perpendicular to \bar{X} . Let (\bar{U}, \bar{V}) be the velocity components in a fixed frame of reference (\bar{X}, \bar{Y}) . It should be noted that $\phi = 0$ corresponds to a symmetric channel with waves out of phase and for $\phi = \pi$ the waves are in phase.

In the laboratory frame (\bar{X}, \bar{Y}) the flow is unsteady. However it is observed in a coordinate system (\bar{x}, \bar{y}) moving at the wave speed C , the flow can be treated as steady. The coordinates and velocities in the wave and lab frames related through the following expressions:

$$\bar{x} = \bar{X} - c\bar{t}, \quad \bar{y} = \bar{Y}, \quad \bar{u}(\bar{x}, \bar{y}) = \bar{U} - c, \quad \bar{v}(\bar{u}, \bar{v}) = \bar{V} \quad (3)$$

where \bar{u} and \bar{v} are the velocity components in the wave frame.

Neglecting body force and body couple, the equations governing the steady flow of an incompressible micropolar fluid in the presence of an external magnetic field, on neglecting the induced magnetic field, are given by

$$\frac{\partial \bar{u}}{\partial x} + \frac{\partial \bar{v}}{\partial y} = 0, \quad (4)$$

$$\rho \left(u \frac{\partial \bar{u}}{\partial x} + v \frac{\partial \bar{u}}{\partial y} \right) = -\frac{\partial \bar{p}}{\partial x} + (\mu + k) \left(\frac{\partial^2 \bar{u}}{\partial x^2} + \frac{\partial^2 \bar{u}}{\partial y^2} \right) + k \frac{\partial \bar{w}}{\partial y} - \frac{\mu}{K} (\bar{u} + c) - \sigma_0 B_0^2 (\bar{u} + c), \quad (5)$$

$$\rho \left(u \frac{\partial \bar{v}}{\partial x} + v \frac{\partial \bar{v}}{\partial y} \right) = -\frac{\partial \bar{p}}{\partial y} + (\mu + k) \left(\frac{\partial^2 \bar{v}}{\partial x^2} + \frac{\partial^2 \bar{v}}{\partial y^2} \right) - k \frac{\partial \bar{w}}{\partial y} - \frac{\mu}{K} \bar{v}, \tag{6}$$

$$\rho \bar{J} \left(u \frac{\partial \bar{w}}{\partial x} + v \frac{\partial \bar{w}}{\partial y} \right) = -2k \bar{w} + \nu \left(\frac{\partial^2 \bar{w}}{\partial x^2} + \frac{\partial^2 \bar{w}}{\partial y^2} \right) + k \left(\frac{\partial \bar{v}}{\partial x} - \frac{\partial \bar{u}}{\partial y} \right), \tag{7}$$

where \bar{u} and \bar{v} are the velocity components in the \bar{x} and \bar{y} directions, respectively, \bar{w} is the microrotation velocity component in the direction normal to both \bar{x} and \bar{y} axes. \bar{p} is the fluid pressure, σ_0 is the electrical conductivity, B_0 is the strength of magnetic field, K is the permeability, μ coefficient of viscosity, k, γ are the viscosity constants of for micropolar fluid, ρ and \bar{J} are the fluid density and microgyration parameter.

For the flow under consideration, the velocity field is $\bar{v} = (\bar{u}, \bar{v}, 0)$ and micro rotation vector is $\bar{w} = (0, 0, w^1)$. We introduce the following non-dimensional quantities:

$$\begin{aligned} x &= \frac{\bar{x}}{\lambda}, & y &= \frac{\bar{y}}{d_1}, & u &= \frac{\bar{u}}{c}, & v &= \frac{\lambda \bar{v}}{d_1 c}, & w &= \frac{d_1 \bar{w}}{c}, & t &= \frac{c}{\lambda} \bar{t}, & j &= \frac{\bar{j}}{d_1^2}, \\ h_1 &= \frac{\bar{h}_1}{d_1}, & h_2 &= \frac{\bar{h}_2}{d_1}, & \delta &= \frac{d_1}{\lambda}, & \text{Re} &= \frac{\rho c d_1}{\mu}, & p &= \frac{d_1^2}{c \lambda \mu} \bar{p}, & K &= \frac{\bar{K}}{d_1^2}, \\ \sigma &= \frac{1}{\sqrt{K}}, & M &= \sqrt{\frac{\sigma_0}{\mu}} d_1 B_0, & a &= \frac{a_1}{d_1}, & b &= \frac{a_2}{d_1} \text{ and } d = \frac{d_2}{d_1} \end{aligned} \tag{8}$$

where Re is the Reynolds number, δ is the dimensionless wave number, σ is the permeability parameter, M is the Hartmann number and p is the pressure.

The governing quantities in dimensionless form can be written as

$$\frac{\partial u}{\partial x} + \frac{\partial u}{\partial y} = 0 \tag{9}$$

$$\text{Re} \delta \left(u \frac{\partial u}{\partial x} + v \frac{\partial u}{\partial y} \right) = -\frac{\partial p}{\partial x} + \frac{1}{1-N} \left(N \frac{\partial w}{\partial y} + \delta^2 \frac{\partial^2 u}{\partial x^2} + \frac{\partial^2 u}{\partial y^2} \right) - (\sigma^2 + M^2)(u+1) \tag{10}$$

$$\text{Re} \delta^3 \left(u \frac{\partial v}{\partial x} + v \frac{\partial v}{\partial y} \right) = -\frac{\partial p}{\partial y} + \frac{\delta^2}{1-N} \left(-N \frac{\partial w}{\partial x} + \delta^2 \frac{\partial^2 v}{\partial x^2} + \frac{\partial^2 v}{\partial y^2} \right) - \delta^2 \sigma^2 v \tag{11}$$

$$\frac{\text{Re} j \delta (1-N)}{N} \left(u \frac{\partial w}{\partial x} + v \frac{\partial w}{\partial y} \right) = -2w + \left(\delta^2 \frac{\partial v}{\partial x} - \frac{\partial u}{\partial y} \right) + \frac{2-N}{m^2} \left(\delta^2 \frac{\partial^2 w}{\partial x^2} + \frac{\partial^2 w}{\partial y^2} \right) \tag{12}$$

where $N = \frac{k}{\mu + k}$, is the coupling number ($0 \leq N \leq 1$), $m^2 = d_1^2 k (2\mu + k) / (\gamma(\mu + k))$ is the micropolar parameter.

Using long wavelength and low Reynolds number approximations, (9) to (12) reduce to

$$\frac{\partial u}{\partial x} + \frac{\partial u}{\partial y} = 0 \tag{13}$$

$$(1-N) \frac{\partial p}{\partial x} = N \frac{\partial w}{\partial y} + \frac{\partial^2 u}{\partial y^2} - (1-N)(\sigma^2 + M^2)(u+1) \tag{14}$$

$$\frac{\partial p}{\partial y} = 0 \tag{15}$$

$$-2w - \frac{\partial u}{\partial y} + \frac{(2-N)}{m^2} \frac{\partial^2 w}{\partial y^2} = 0 \tag{16}$$

The corresponding non-dimensional boundary conditions in the wave frame are

$$\begin{aligned} u &= -1 & \text{at} & \quad y = h_1 \text{ and } h_2 \\ w &= 0 & \text{at} & \quad y = h_1 \text{ and } h_2 \end{aligned} \tag{17}$$

The dimensional volume flow rate in the laboratory frame is

$$Q = \int_{\bar{h}_2(\bar{x}, \bar{t})}^{\bar{h}_1(\bar{x}, \bar{t})} \bar{U}(\bar{X}, \bar{Y}, \bar{t}) d\bar{Y} \tag{18}$$

In the wave frame the above equation reduces to

$$q = \int_{\bar{h}_2(\bar{x})}^{\bar{h}_1(\bar{x})} \bar{u}(\bar{x}, \bar{y}) d\bar{y} \tag{19}$$

From equations (3), (18) and (19), we get

$$Q = q + c\bar{h}_1(\bar{x}) - c\bar{h}_2(\bar{x}) \tag{20}$$

The time averaged flow over a period T at a fixed position \bar{X} is

$$\bar{Q} = \frac{1}{T} \int_0^T Q dt \tag{21}$$

Using (20) in (21) and then integrating we get

$$\bar{Q} = q + cd_1 + cd_2 \tag{22}$$

Defining the dimensionless mean flow Θ in the laboratory frame and F in the wave frame as

$$\Theta = \frac{\bar{Q}}{cd_1}, \quad F = \frac{q}{cd_1} \tag{23}$$

Equation (22) reduces to

$$\Theta = F + 1 + d \tag{24}$$

in which

$$F = \int_{h_2}^{h_1} u \, dy \tag{25}$$

where $h_1(x) = 1 + a \cos(2\pi x)$, $h_2(x) = -d - b \cos(2\pi x + \phi)$

3. Solution of the problem

By differentiating equation (16) with respect to y and then using in equation (14) we obtain

$$(N-2) \frac{\partial w}{\partial y} + \frac{(2-N)}{m^2} \frac{\partial^3 w}{\partial y^3} - (1-N)(\sigma^2 + M^2)(u+1) = (1-N) \frac{\partial p}{\partial x}$$

On simplification we get

$$u = \frac{1}{(1-N)(\sigma^2 + M^2)} \left[(N-2) \frac{\partial w}{\partial y} + \frac{(2-N)}{m^2} \frac{\partial^3 w}{\partial y^3} - (1-N) \frac{\partial p}{\partial x} \right] - 1 \tag{26}$$

using equation (26) in (16) we obtain

$$\frac{\partial^4 w}{\partial y^4} - \frac{\partial^2 w}{\partial y^2} A + wB = 0 \tag{27}$$

the general solution of equation (27) is given by

$$w = c_1 \cosh \theta_1 y + c_2 \sinh \theta_1 y + c_3 \cosh \theta_2 y + c_4 \sinh \theta_2 y \tag{28}$$

where $\theta_1 = \sqrt{\frac{A + \sqrt{A^2 - 4B}}{2}}$, $\theta_2 = \sqrt{\frac{A - \sqrt{A^2 - 4B}}{2}}$

$$A = (1-N)(\sigma^2 + M^2) + m^2, \quad B = 2m^2(1-N)(\sigma^2 + M^2)/(2-N)$$

Substituting (27) in (25) we get

$$u = L_1 (c_1 \sinh \theta_1 y + c_2 \cosh \theta_1 y) + L_2 (c_3 \sinh \theta_2 y + c_4 \cosh \theta_2 y) - \frac{1}{(\sigma^2 + M^2)} \frac{\partial p}{\partial x} - 1 \tag{29}$$

The arbitrary constants C_1, C_2, C_3 and C_4 are obtained by applying the boundary conditions (17) and they are presented below

$$c_1 = L_{19} \frac{dp}{dx}, c_2 = L_{20} \frac{dp}{dx}, c_3 = L_{21} \frac{dp}{dx}, c_4 = L_{22} \frac{dp}{dx}$$

From equation (25) we find that

$$\frac{dp}{dx} = \frac{F + (h_1 - h_2)}{L_{23} + L_{24} - L_{25}} \tag{30}$$

where $F = \Theta - 1 - d$

The non-dimensional form of the pressure rise per wavelength ΔP is given by

$$\Delta p = \int_0^1 \left(\frac{dp}{dx} \right) dx \tag{31}$$

An important property of the micropolar fluid is that the stress tensor is not symmetric. The non-dimensional shear stresses in the problem under consideration are given by

$$\tau_{xy} = \frac{\partial u}{\partial y} - \frac{N}{1-N} w \tag{32}$$

$$\tau_{yx} = \frac{1}{1-N} \frac{\partial u}{\partial y} + \frac{N}{1-N} w \tag{33}$$

RESULTS AND DISCUSSION

Equation (29) gives the expression for velocity as a function of y . The velocity profiles are plotted in figures from (1) to (5) to study the effects of different parameters such as coupling number N , microrotation parameter m , permeability parameter σ , phase difference ϕ , and magnetic parameter M on the velocity distribution in the asymmetric channel. Figures 1 and 2 are plotted for different values of coupling number N and microrotation parameter m . It is observed that velocity profiles are parabolic. Also we noticed that the velocity decreases with increasing N whereas it increases for increasing microrotation parameter m . Figures 3 and 4 depict that the increase in magnetic parameter M and permeability parameter σ reduces the velocity in the mid way of the channel. Further from figure 5 it can be found that the velocity decreases with increasing ϕ .

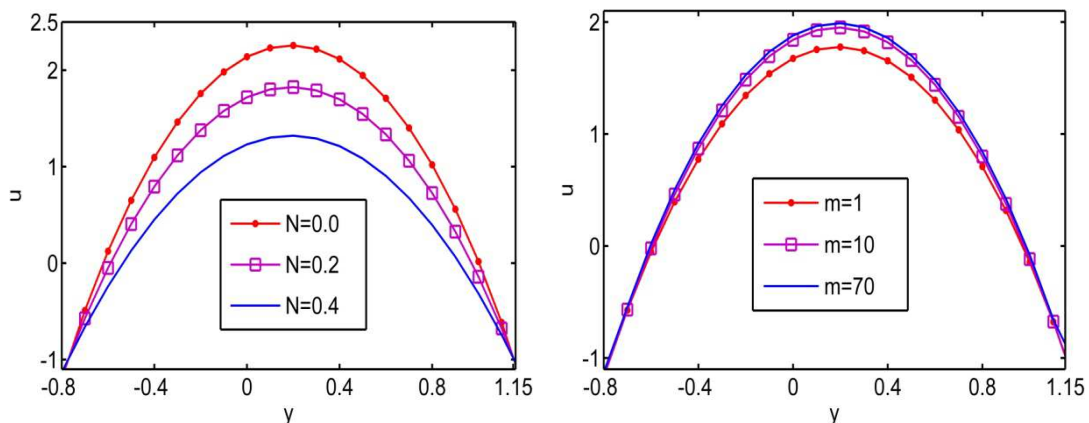


Fig.1 Velocity profiles for different 'N' with fixed : $a = 0.5, b = 0.5,$

$d = 1, x = 0.2, \phi = \pi/4, m = 2, dp / dx = -10, \sigma = 0.4, M = 1.$

Fig.2 Velocity profiles for different 'm' with fixed : $a = 0.5, b = 0.5,$

$d = 1, x = 0.2, \phi = \pi/4, N = 0.2, dp / dx = -10, \sigma = 0.4, M = 1.$

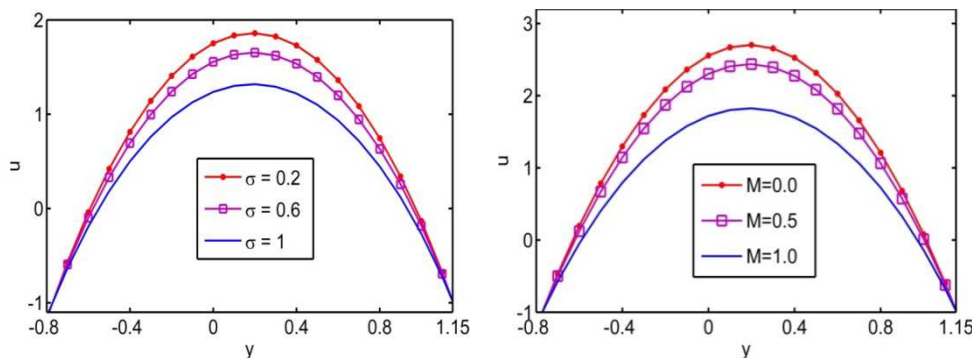


Fig.3 Velocity profiles for different ‘ σ ’ with fixed : $a=0.5, b=0.5,$

$d=1, x = 0.2, \phi = \pi/4, m=2, N=0.2, dp/dx = -10, M=1$

Fig.4 Velocity profiles for different ‘ M ’ with fixed : $a=0.5, b=0.5,$

$d=1, x = 0.2, \phi = \pi/4, m=2, N=0.2, dp/dx = -10, \sigma=0.4$

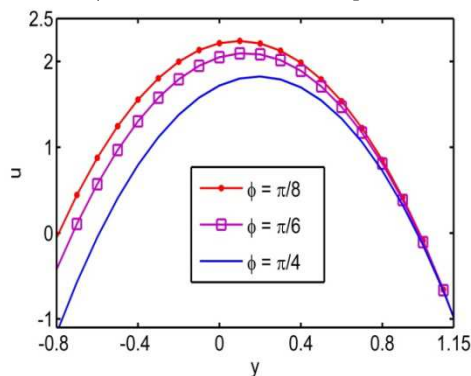


Fig.5 Velocity profiles for different ‘ ϕ ’ with fixed : $a=0.5, b=0.5,$

$d=1, x = 0.2, m=2, N=0.2, dp/dx = -10, \sigma=0.4, M=1.$

The expression for the pressure gradient dp/dx is given by equation (30). The variation of pressure gradient with the wave length for different values of coupling number N and microrotation parameter m is shown in figures 6 and 7. It is observed that in the wider part of the channel the pressure gradient is relatively small while in a narrow part of the channel a much pressure gradient is required to maintain the flux. On other wards the magnitude of the pressure gradient increases with increasing N where as it decreases with increasing m . From figures 8 and 9 we observe that dp/dx increases with increasing Magnetic parameter M and permeability parameter σ . Figure 10 depicts that the amplitude of the pressure gradient decreases with increasing ϕ .

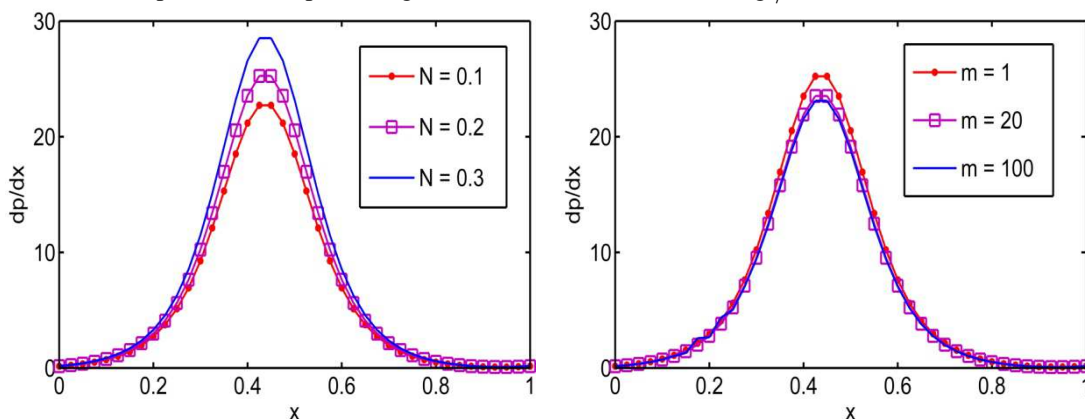


Fig.6 Variation of pressur gradient versus wavelength for different ‘ N ’ with

fixed : $a=0.5, b=0.5, d=1, \phi = \pi/4, m=0.5, \sigma = 0.3, M=1, \Theta=-1$

Fig.7 Variation of pressur gradient versus wavelength for different ‘ m ’ with

fixed : $a=0.5, b=0.5, d=1, \phi = \pi/4, N=0.2, \sigma = 0.3, M=1, \Theta=-1$

The equation (31) gives the expression for the pressure rise Δp in terms of the mean flow Θ . The variation of pressure rise with the mean flow for different values of coupling number N is shown in figure 11. It is observed that the pressure rise increases with increasing N and the pumping curves meet at the point (0.6, 0). Further apposite behavior is observed. Figure 12 shows that the pressure rise increases with decreasing microrotation parameter m and the pumping curves are intersect at the point (0.6, 0). After this point situation is reversed. From figures 13 and 14 we noticed that the pressure rise increases with increasing permeability parameter σ and Magnetic parameter M and the pumping curves are meet at $\Theta = 0.2$. Further apposite behavior is observed. Figure 15 depicts that the pressure rise decreases with increasing phase difference ϕ .

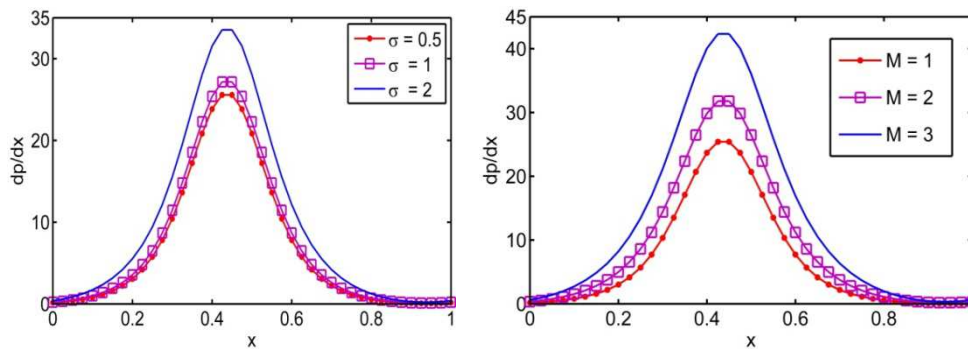


Fig.8 Variation of pressur gradient versus wavelength for different ' σ ' with fixed : $a = 0.5, b = 0.5, d = 1, \phi = \pi / 4, N = 0.2, m = 0.5, M = 1, \Theta = -1$

Fig.9 Variation of pressur gradient versus wavelength for different ' M ' with fixed : $a = 0.5, b = 0.5, d = 1, \phi = \pi / 4, N = 0.2, m = 0.5, \sigma = 0.3, \Theta = -1$

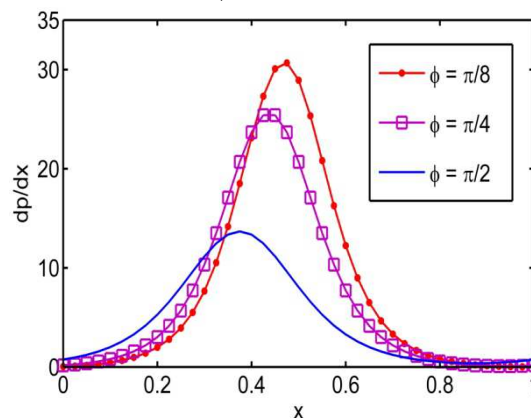


Fig.10 Variation of pressur gradient versus wavelength for different ' ϕ ' with fixed : $a = 0.5, b = 0.5, d = 1, N = 0.2, m = 0.5, \sigma = 0.3, M = 1, \Theta = -1$

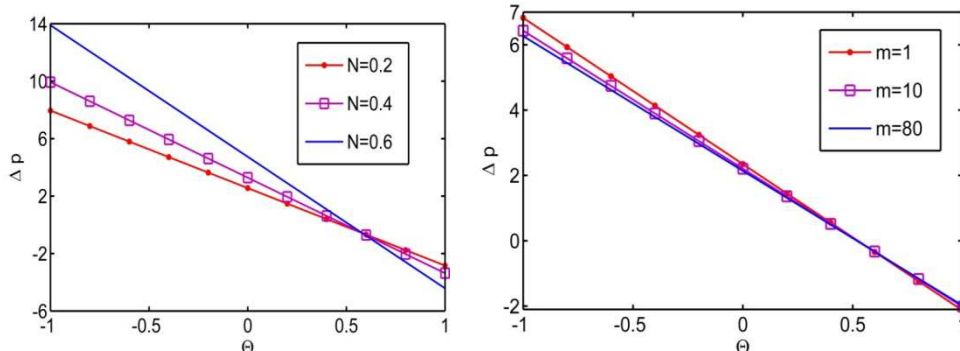


Fig.11 Variation of pressurerise versus flow rate for different ' N ' with fixed : $a = 0.5, b = 0.5, d = 1, \phi = \pi / 4, m = 0.5, \sigma = 0.4, M = 1.5$

Fig.12 Variation of pressurerise versus flowrate for different ' m ' with fixed : $a = 0.5, b = 0.5, d = 1, \phi = \pi / 4, N = 0.2, \sigma = 0.3, M = 1$

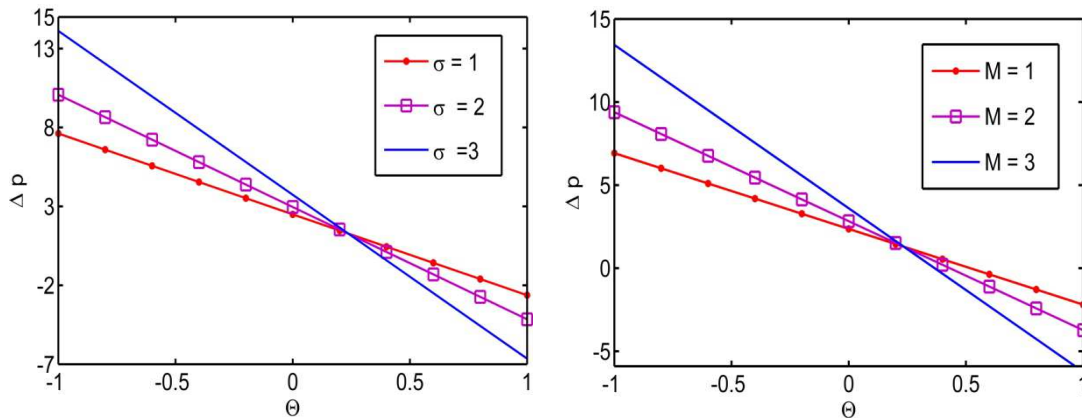


Fig.13 Variation of pressurerise versus flowrate for different ‘σ’ with fixed : a = 0.5, b = 0.5, d = 1, φ = π / 4, N = 0.2, m = 0.5, M = 1

Fig.14 Variation of pressurerise versus flowrate for different ‘M’ with fixed : a = 0.5, b = 0.5, d = 1, φ = π / 8, N = 0.2, m = 0.5, σ = 0.4

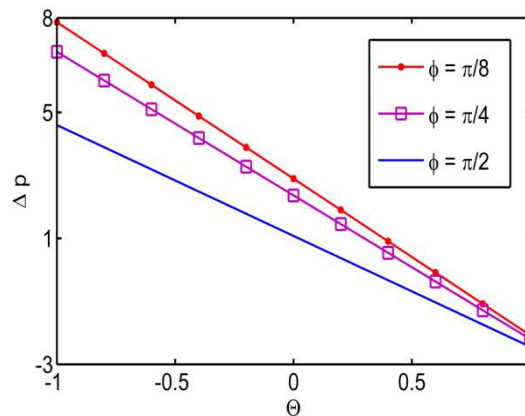


Fig.15 Variation of pressurerise versus flowrate for different ‘φ’ with fixed : a = 0.5, b = 0.5, d = 1, N = 0.2, m = 0.5, σ = 0.4, M = 1

Appendix

$$L_1 = \frac{(N-2)\theta_1(1-\frac{\theta_1^2}{m^2})}{(1-N)(\sigma^2 + M^2)}, L_2 = \frac{(N-2)\theta_2(1-\frac{\theta_2^2}{m^2})}{(1-N)(\sigma^2 + M^2)},$$

$$L_3 = \frac{(\cosh \theta_2 h_2 - \cosh \theta_2 h_1)}{(\sigma^2 + M^2)}, L_4 = L_1 (\sinh \theta_1 h_1 \cosh \theta_2 h_2 - \sinh \theta_1 h_2 \cosh \theta_2 h_1)$$

$$L_5 = L_1 (\cosh \theta_1 h_1 \cosh \theta_2 h_2 - \cosh \theta_1 h_2 \cosh \theta_2 h_1),$$

$$L_6 = L_2 (\sinh \theta_2 h_1 \cosh \theta_2 h_2 - \sinh \theta_2 h_2 \cosh \theta_2 h_1),$$

$$L_7 = (\cosh \theta_1 h_1 \sinh \theta_2 h_2 - \cosh \theta_1 h_2 \sinh \theta_2 h_1),$$

$$L_8 = (\sinh \theta_1 h_1 \sinh \theta_2 h_2 - \sinh \theta_1 h_2 \sinh \theta_2 h_1),$$

$$L_9 = (\cosh \theta_2 h_1 \sinh \theta_2 h_2 - \cosh \theta_2 h_2 \sinh \theta_2 h_1),$$

$$L_{10} = (L_1 \sinh \theta_1 h_1 \sinh \theta_2 h_1 - L_2 \cosh \theta_1 h_1 \cosh \theta_2 h_1),$$

$$L_{11} = (L_1 \cosh \theta_1 h_1 \sinh \theta_2 h_1 - L_2 \sinh \theta_1 h_1 \cosh \theta_2 h_1),$$

$$L_{12} = L_2(\sinh^2 \theta_2 h_1 - \cosh^2 \theta_2 h_1), L_{13} = \frac{dp}{dx} \frac{\sinh \theta_2 h_1}{(\sigma^2 + M^2)}$$

$$L_{14} = L_4 L_9 - L_6 L_7, L_{15} = L_5 L_9 - L_6 L_8, L_{16} = L_3 L_{12} - L_6 L_{13},$$

$$L_{17} = L_4 L_{12} - L_6 L_{10}, L_{18} = L_5 L_{12} - L_6 L_{11}, L_{19} = \frac{L_3 L_9 L_{18} - L_{15} L_{16}}{L_{14} L_{18} - L_{15} L_{17}}$$

$$L_{20} = \frac{L_3 L_9 - L_{19} L_{14}}{L_{15}}, L_{21} = \frac{L_{13} - L_{19} L_{10} - L_{20} L_{11}}{L_{12}},$$

$$L_{22} = \frac{\frac{1}{(\sigma^2 + M^2)} - L_{19} L_1 \sinh \theta_1 h_2 - L_{20} L_1 \cosh \theta_1 h_2 - L_{21} L_2 \sinh \theta_2 h_2}{L_2 \cosh \theta_2 h_2}$$

$$L_{23} = \frac{L_1}{\theta_1} [L_{19}(\cosh \theta_2 h_1 - \cosh \theta_1 h_2) + L_{20}(\sinh \theta_1 h_1 - \sinh \theta_1 h_2)],$$

$$L_{24} = \frac{L_2}{\theta_2} [L_{21}(\cosh \theta_2 h_1 - \cosh \theta_2 h_2) + L_{22}(\sinh \theta_2 h_1 - \sinh \theta_2 h_2)]$$

$$L_{25} = \frac{(h_1 - h_2)}{(\sigma^2 + M^2)}$$

REFERENCES

- [1] A.C. Eringen, *J. Math. Mech.*, **1966**, 16, 1-16.
- [2] G. Lukaszewicz, Birkhauser, Boston., **1999**.
- [3] D. Srinivasacharya, M. Mishra, A.R. Rao, *Acta. Mech.*, **2003**, 161, 165-178.
- [4] N. Ali, T. Hayat, *Computers and Mathematics with applications*, **2008**, 55, 589-608.
- [5] T. Hayat, N. Ali, Z. Abbas, *Phys. Lett. A*, **2008**, 370, 331-334.
- [6] S. Sreenadh, P. Lakshminarayana, G. Sucharitha, *Int. J. of Appl. Math. and Mech.*, **2011**, 7(20), 18- 37.
- [7] M. Arun Kumar, S. Venkataramana, S. Sreenadh, P. Lakshminarayana, **2012**, 3 (11), 4004-4016.
- [8] Kh.S. Mekheimer, *Appl. Math. Comput.*, **2004**, 153, 763-777.
- [9] M. Kothandapani, S. Srinivas, *Int. J. Nonlinear Mech.*, **2008**, 43, 915-924.
- [10] T. Hayat, N. Ali, *Commun. Nonlinear Sci. Num. Simul.*, **2008**, 13(7), 1343-1352.
- [11] Kh.S. Mekheimer, Y. ABD Elmaboud, *Phys. Lett.*, **2008**, A 372, 1657-1665.
- [12] S. Noreen, T. Hayat, A. Alsaedi, *Int. J. Phys. Sci.*, **2011**; 6: 8018-8026.
- [13] P. Lakshminarayana, S. Sreenadh, G. Sucharitha, *Advances in applied science research*, **2012**, 3 (5), 2890-2899.
- [14] P. Lakshminarayana, S. Sreenadh, G. Sucharitha, *Procedia Engineering*, **2015**, 127, 1087-1094.
- [15] K. Vajravelu, S. Sreenadh, G. Sucharitha, P. Lakshminarayana, *International Journal of Biomathematics*, **2014**, 7 (6), 1450064 (25 pages).
- [16] S. Sreenadh, P. Lakshminarayana, M. Arun kumar, G. Sucharitha, *International Journal of Mathematical Sciences and Engineering Applications (IJMSEA)*, **2014**, 8 (V), 27-40.
- [17] S. Srinivas, M. Kothandapani, *Appl. Math. Comput.*, **2009**, 213, 197-208.
- [18] G. Sucharitha, S. Sreenadh, P. Lakshminarayana, *Int. J. of Eng. Research & Technology*, **2012**, 1(10), 1-10.
- [19] M. Mishra, A. Ramachandra Rao, *J. Non-Newtonian Fluid Mech.*, **2004**, 121 , 163-74.
- [20] K. Vajravelu, S. Sreenadh, P. Lakshminarayana, *Commun. Non- linear Sci. Numer. Simulat.*, **2011**, 16, 3107-3125.
- [21] P. Lakshminarayana, S. Sreenadh, G. Sucharitha, *Advances In Applied Science Research*, **2015**, 6 (2), 107-118.
- [22] S. Sreenadh, P. Lakshminarayana, V. Jagadesh, G. Sucharitha, K. Nandagopal, *Global Journal of Pure and Applied Mathematics*, **2015**. 11 (2), 851-866.
- [23] K. Vajravelu, S. Sreenadh, P. Lakshminarayana, G. Sucharitha, *International Journal of Biomathematics*, **2016**, 9 (2), 1650023(25 pages).